

Research article

Impact of urban morphology on the spatial and temporal distribution of PM_{2.5} concentration: A numerical simulation with WRF/CMAQ model in Wuhan, China



Huahua Xu ^a, Hong Chen ^{b,*}

^a School of Architecture and Urban Planning, Huazhong University of Science and Technology, Wuhan, 430074, China

^b School of Architecture and Urban Planning, Huazhong University of Science and Technology, Hubei Engineering and Technology Research Center of Urbanization, Wuhan, 430074, China

ARTICLE INFO

Keywords:

Urban morphology
Numerical simulation
PM_{2.5} concentration
Spatiotemporal distribution

ABSTRACT

The urban morphology can significantly change the urban microclimate, which in turn affects the diffusion of air pollutants. Urban planning is the most important means of shaping urban morphology. Therefore, this study takes Wuhan as an example and uses the method of WRF/CMAQ coupled UCM model to analyze the spatial and temporal distribution characteristics of PM_{2.5} in the Wuhan metropolitan area in winter 2015. The six most important urban morphological indicators in urban planning: the floor area ratio and building height, building density and building width, vegetation coverage ratio, and urban fraction, are selected and classified into three groups. Studying their impact on the spatial and temporal distribution of PM_{2.5} concentration provides support for urban planners to improve air quality. The results show that the maximum value of PM_{2.5} concentration in Wuhan urban area occurs in the morning rush hour, and PM_{2.5} is distributed concentrically in the downtown of the city (within the second ring highway) according to the highways around the city. The PM_{2.5} concentration in the downtown area with the most extensive urban morphological index is the highest, and it decreases with increasing distance from the downtown. Among the six indicators, building density and urban fraction have the most significant impact on PM_{2.5} concentration because they have the greatest impact on the wind speed at 10 m. The height of the planetary boundary layer is the key factors affect the vertical and horizontal diffusion of air pollutants. Except for the vegetation coverage ratio, the increase of other urban morphological indicators will lead to a decrease of PM_{2.5} concentration in Wuhan urban area at night. During the daytime, increasing the floor area ratio and building height will cause an increasing of PM_{2.5} concentration, but other indicators have the opposite effects.

1. Introduction

With the urbanization process, the urban heat island effect and air pollution have become the main environmental problems of most cities in China. They not only increase the urban air conditioning load and energy consumption but also cause extreme weather events such as heat-waves and smog in the city. In severe cases, they even endanger the health of residents (Buckley et al., 2012; Huang et al., 2019), and greatly increase the risk of children suffering from respiratory diseases (Chen et al., 2014).

Previous studies have shown that there are many factors that affect the PM_{2.5} concentration, including geographic factors, meteorological factors, and artificial factors. Complex terrain conditions will change the

local air temperature, wind speed and direction, which will affect the diffusion of pollutants (Kang et al., 2012; Tham et al., 2019). A large number of studies have shown that the trees not only have a good cooling effect by transpiration (Chen et al., 2019b), but also have strong adsorption of toxic gases and particle matters in the atmosphere through their leaves, and the capacity of this adsorption depends on the type of plant, canopy size of the trees, leaf area index, etc. (Saebo et al., 2012; Rasanen et al., 2013; Wang et al., 2015). Rivers and lakes in the city as a "cold source" can not only effectively reduce the air temperature and alleviate the urban heat island effect (Gunawardena et al., 2017), but also increase the relative humidity of the air. This will increase the weight and surface adsorption of particulate matter, and promote the dry and the wet deposition of particulate matter, thereby reducing the

* Corresponding author.

E-mail addresses: d201577762@hust.edu.cn (H. Xu), chhwh@hust.edu.cn (H. Chen).

concentration of particulate matter in the atmosphere (Zeng et al., 2017). The meteorological factors that affect PM_{2.5} concentration mainly include atmospheric circulation, the height of the planetary boundary layer, air temperature, relative humidity, wind speed and direction. Atmospheric circulation, boundary layer height and wind speed can affect the horizontal and the vertical diffusion of particles (Wang et al., 2014; Hu et al., 2016; Banks and Baldasano, 2016). Air temperature can change the photochemical reaction rate of air pollutants, accelerating or slowing down the formation process of air pollutants (Tai et al., 2010; Aw and Kleeman, 2003). Relative humidity of the air will affect the dry and the wet deposition rate of particulate matter (Dawson et al., 2007; He and Lin, 2017).

In addition to natural factors, human activities will also have a decisive impact on PM_{2.5} concentration. For example, industrial emissions, transportation emissions, and residential emissions are the three main sources of urban anthropogenic heat and air pollutants (Ohara et al., 2007; Aldabe et al., 2011), and they are decisive for the concentration and spatial distribution of air pollutants. The size of the city (Shi et al., 2019b), compactness (Ma et al., 2015; Chen et al., 2011; Ou et al., 2013), building height (BH), building density (BD) (Guo et al., 2019), and vegetation coverage (VC) (Shi et al., 2019a; Chen et al., 2019a) and other morphological factors will affect air temperature, humidity, and ventilation, which will affect the diffusion, migration, and sedimentation of pollutants. Based on the research of Buyantuyev et al. (2010), Shi et al. (2019a) proposed six indicators: total urban area, number of patches, landscape shape index, percentage of like adjacencies, patch cohesion index, and aggregation index to represent the urban morphology. Yin et al. (2018) used the other three indicators: the sky view fraction (SVF), BD, and FAR related to affecting the urban heat island. Moreover, for the same purpose, Zhou et al. (2017) used three other indicators: urban built-up area, fractal dimension, and centripetal anisometry. In China, the most influential and most concerned urban morphological indicators are FAR, BD, VC, BH, building width(BW), road width(RW), which are close connected with each other. FAR is directly related to BH; when the BD is constant, FAR increases with the BH. BD is affected by the BW and RW, which is proportional to the BW and is inversely proportional to the RW. VC has a negative correlation with UF which means the area ratio of an urban impervious surface. Most Chinese urban planners have not considered their impact on the urban microclimate when formulating those urban morphological indicators, so we selected six indicators that are most commonly used in urban planning: FAR, BD, VC, BH, BW, urban fraction(UF). Those six indicators were divided into three groups according to their mutual relationship, namely FAR and BH, BD and BW, VC and UF.

The earliest research on air pollution problems was meteorology and environmental engineering, focusing on the physical and chemical processes of various components in the atmosphere, including the emission, diffusion, and chemical reactions of air pollutants (Tai et al., 2010; Dawson et al., 2007). The method mainly adopts numerical simulation methods. Usually, it is necessary to couple the weather model such as WRF and MM5, with the air quality model (CMAQ, CAMx, etc.). Due to the massive scope in these two fields, the resolution of the simulation ranges from several kilometers to tens of kilometers, and the heterogeneity of complex urban forms are usually ignored, and the city is only abstracted into a single homogeneous box. At present, urban air quality research in the fields of architecture and urban planning mainly focuses on the micro-scale block scale, and the grid accuracy is usually a few meters to tens of meters. This type of research focuses on the influence of factors such as the building form (Chen and Yang, 2019), building layout, the interface form of enclosed streets valleys, vegetation coverage (Jeanjean et al., 2016) on the diffusion of pollutants in the neighborhood(Shi et al., 2016). The advantage of this type of research is that it can accurately study the changes of the pollutants concentration in the street canyon and the factors that causing the concentration change. However, its disadvantage is that the research scope is too small, generally only about 1 km, lacking the grasp of the overall spatial

form and climate characteristics of the city, and it is impossible to calculate the transfer of pollutants in a larger area.

This article selects six urban morphological indicators of FAR, BH, BD, BW, VC and UF from the perspective of urban planning, and uses the WRF/CMAQ coupling method to study their impact on the temporal and spatial distribution of PM_{2.5} concentration, and provide urban planning strategies for improving air quality.

2. Data and methods

2.1. The numerical model of WRF/UCM coupling CMAQ

The WRF (Weather Research and Forecast) model is a new generation of non-static, high-resolution and fully compressible mesoscale atmospheric forecasting model jointly developed by the National Center for Atmospheric Research (NCAR), National Center for Environmental Prediction (NCEP), etc. The WRF model uses completely non-static governing equations, including various physical equations such as atmospheric horizontal and vertical diffusion equations, solar short-wave radiation scheme, long-wave radiation scheme, land surface process parameterization scheme, cloud microphysical parameterization scheme, etc. The WRF model can output meteorological parameters with coordinate such as air temperature, relative humidity, atmospheric pressure, solar radiation, and long-wave radiation gained and lost on the surface and mainly used to simulate various meteorological processes and phenomena. As we all know, the complex urban form and a large number of artificial underlying surfaces have disrupted the water vapor and energy balance between the ground and the atmosphere, resulting in an urban microclimate that is different from the rural. In order to better describe the form and physical properties of the city, Masson (2000), Kusaka et al. (2001); Kusaka and Kimura (2004) proposed the single-layer urban canopy model (UCM), which was later improved by Chen et al. (2004), Miao et al. (2009) and coupled to the WRF model. This study introduced the single-layer urban canopy model (UCM, Supplementary Fig. S1), which can improve the accuracy of the simulation results for CMAQ (Kang et al., 2016). The main parameters that describe the urban morphology in the UCM are building height (Roof_level), building width (Roof_width), road width (Road_width), and an urban fraction (the urban impervious surface except for greening). Those parameters can well correspond with the urban morphological indicators mentioned above, and the following formulas can express the mutual relationship between them:

$$R = \frac{Roof_width}{Roof_width + Road_width} \quad (1)$$

$$FAR = \frac{ZR \cdot R^2}{3} \quad (2)$$

$$Building_density = FRC_URB \cdot R \quad (3)$$

$$FRC_URB = 1 - FRC_GREEN \quad (4)$$

Where R represents the proportion of buildings in the urban built-up area, Roof_width represents the average width of the buildings, Road_width represents the average width of the roads, FAR represents the floor area ratio, ZR represents the average building height, Building_density represents the average building density, FRC_URB represents the proportion of the urban impervious surface, and FRC_GREEN represents the vegetation coverage ratio.

The CMAQ (Community Multi-scale Air Quality Modeling System) is a third-generation air quality model developed by the U.S. Environmental Protection Agency (USEPA). It is based on the concept of "one atmosphere" and unifies a variety of atmospheric pollutants into an atmospheric model. It includes an initial condition processor (ICON), a boundary condition processor (BCON), photolysis rate processor (JPROC), meteorology-chemistry interface processor (MCIP), and

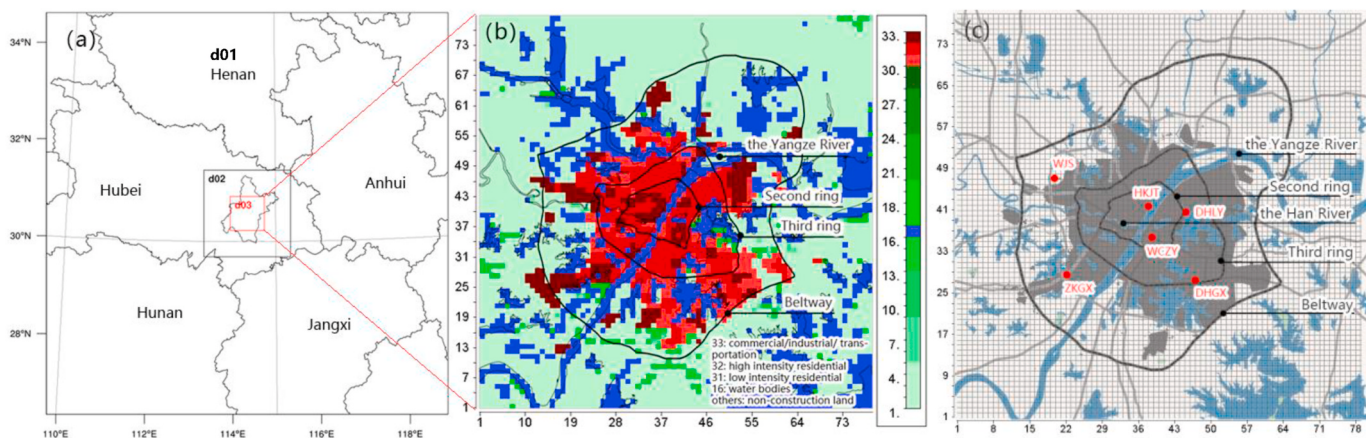


Fig. 1. (a) Simulation scope for the WRF model, (b) Spatial pattern of Wuhan urban area and land use classified as USGS classification,(c) National environmental monitoring stations.

CMAQ chemistry-transport model (CCTM), which are mainly used to simulate the gas phase chemical process, aerosol chemical and power process, and transmission of atmospheric pollutants And diffusion process, etc. CMAQ cannot independently calculate the complicated meteorological change process, and requires the WRF mode to provide it with an initial meteorological field.

2.2. Data and material

The numerical model of WRF/UCM coupled CMAQ model were used to simulate the temporal and spatial distribution of PM_{2.5} concentration in this study. There are three main types of data required for simulation, they are initial meteorological data, geographic data and emission inventory. The meteorological inputs were generated with initial and boundary conditions from the National Center for Environmental Prediction (NCEP) final analysis (FNL) data with 6h interval, $1^\circ \times 1^\circ$ spatial resolution. The geographic data used for d01 and d02 was downloaded from the United States Geological Survey (USGS) with 30'' spatial resolution. High-resolution land use and topographic GIS data with a spatial resolution of 30 m were used for d03 provided by Wuhan Natural Resources and Planning Bureau (WNRPB). Since the WRF/UCM model divides the built-up area into three types of construction intensity (industrial/commercial/transportation area, high-intensity residential areas, and low-density residential areas), the different land types in the built-up area of Wuhan are rezoned according to the above three categories. This study reorganized the land in Wuhan's built-up area based on the "Urban Land Use Intensity Division of Wuhan" released by WNRPB (Supplementary Figs. S2 and S3). The emission inventory was obtained from the multi-resolution emission inventory for China (MEIC) compiled by Tsinghua University (<http://www.meicmodel.org/>). Since the emission inventory provided by MEIC failed to meet the requirements for CMAQ simulation in terms of temporal and spatial resolution, we used Python to refine the emission inventory to a spatial resolution of 1-km and a temporal resolution of 1 h according to the method proposed by He et al. (2017). Supplementary Fig. S4 shows the spatial distribution of major air pollutants in Wuhan from emission inventory of MEIC at several typical moments. It can be seen from the figure that the main particulate matter (PM_{2.5}, PMC, etc.) and gaseous pollutants (NH₃, SO₂, CO, NO₂) have the highest emission intensity at 07:00 and 20:00, which are coincide with peak time in the morning and evening in Wuhan. The main emission sources of particulate matter come from central urban areas within the second ring highway and some industrial areas. Similar to particulate matter, gaseous pollutants are distributed along major roads in addition to emission sources in central urban areas.

2.3. Study area and case settings

This study takes the Wuhan metropolitan area as the research scope. Wuhan ($29^{\circ}58'N - 31^{\circ}22'N, 113^{\circ}41'E - 115^{\circ}05'E$) with flat terrain in the urban area, is the largest city in central China with a 10.6 million population and 863 km² urban area by the end of 2015 (Wuhan Statistical Yearbook 2016). The two rivers, the Yangtze River and the Han River met at the center of the city and formed many lakes in the urban area. The built-up area of the city has an obvious concentric structure, and the city is divided into different areas by circular highways. The downtown area of the city locates within the second ring highway, the functions of which are commercial, office, and high-rise residential buildings. This area has the biggest floor area ratio and BD compared with the other areas of the city, as well as the highest average BH in this area (Supplementary Fig. S5). Zones within the third ring highway is the main urban area, with the main function of commercial and residential, and with the second-highest urban morphological indicators in this area. Due to the impact of rapid urbanization, most of the residential buildings in the area are high-rise buildings and even skyscrapers. The region between the third ring highway and the beltway has the lowest urban morphological indicators and has a large number of scattered industrial areas, which is the major industrial emission source of the city.

The computational domain in the WRF model consists of three nested domains (Fig. 1), the grid accuracy is 9 km (d01, 78 × 78 arrays, covering most part of Central China), 3 km (d02, 78×78 arrays, covering Wuhan and its surroundings), 1 km (d03, 78×78 arrays, covering Wuhan Metropolitan area) from the outer layer to the inner layer respectively. The physical options of the WRF mode were chosen as following: the WRF Single-Moment 6-Class (WSM6) scheme for micro-physics (Hong and Lim, 2006); the Yonsei University (YSU) PBL scheme for planetary boundary layer (Hong et al., 2006); the RRTM long-wave and short-wave radiation scheme (Mlawer et al., 1997); the Noah-LSM for land surface model (Chen and Dudhia 2001). The simulation started at 2015-12-24-00:00:00 LST (all times in the text refer to local standard time, LST) and end at 2015-12-31-00:00:00. The CMAQ model contains two levels of nested domains: a coarse domain with 3-km grids, 66 × 66 arrays, and a nested fine domain with 1-km grids, 66 × 66 arrays.

Four scenarios were designed (CASE0 is the basic case) to discuss the impact of the FAR and BH (CASE1), BD and BW (CASE2), VC and UF (CASE 3) on the spatial and temporal distribution of PM_{2.5} concentration. For detailed parameter settings, see Table 2 in section 4.

Table 1

Correlation coefficient (R), mean error (ME), root mean square error (RMSE) of simulated value and observed value of average PM2.5 concentration at 6 stations. T2 means the air temperature at 2 m, U10 means the wind speed at 10 m.

Weather stations	T2			U10			PM2.5		
	R	ME	RMSE	R	ME	RMSE	R	ME	RMSE
HKJT	0.963	0.829	0.961	0.681	1.18	1.37	0.678	11.9	12.7
WCZY	0.917	1.053	1.368	0.681	1.22	1.35	0.719	10.9	14.7
WJS	0.958	0.723	0.928	0.887	2.02	2.21	0.655	14.7	18.2
DHLY	0.966	0.82	0.922	0.815	1.49	1.63	0.738	14.3	17.4
DHGX	0.942	1.642	1.93	0.849	0.37	0.66	0.713	9.2	11.5
ZKXQ	0.957	0.631	0.798	0.818	0.91	1.02	0.736	7.3	8.4

Table 2

Main parameter settings of the four cases. In the table, LR, HR, C/I represent the low-density residential area, the high-density residential area, and the commercial/industrial area respectively, and FAR, BH, BD, BW, VC, UF represent floor area ratio, building height, building density, building width, vegetation coverage and urban fraction.

CASE1 : Floor Area Ratio and Building Height												
Parameters	CASE1-1			CASE1-2			CASE1-3			CASE0		
	LR	HR	C/I	LR	HR	C/I	LR	HR	C/I	LR	HR	C/I
FAR	1.0	2.0	3.0	2.0	3.0	4.0	2.5	3.5	4.5	1.5	2.5	3.5
BH	5	10	15	25	30	35	35	40	45	15	20	25
CASE2 : Building Density and Building Width												
Parameters	CASE2-1			CASE2-2			CASE2-3			CASE0		
	LR	HR	C/I	LR	HR	C/I	LR	HR	C/I	LR	HR	C/I
BD	15	25	35	35	45	55	45	55	65	25	35	45
BW	5	10	15	25	30	35	35	40	45	15	20	25
CASE3 : Vegetation Coverage and Urban Fraction												
Parameters	CASE3-1			CASE3-2			CASE3-3			CASE0		
	LR	HR	C/I	LR	HR	C/I	LR	HR	C/I	LR	HR	C/I
VC	45	35	25	25	15	5	20	10	0	35	25	15
UF	0.45	0.55	0.65	0.65	0.75	0.85	0.75	0.85	0.95	0.55	0.65	0.75

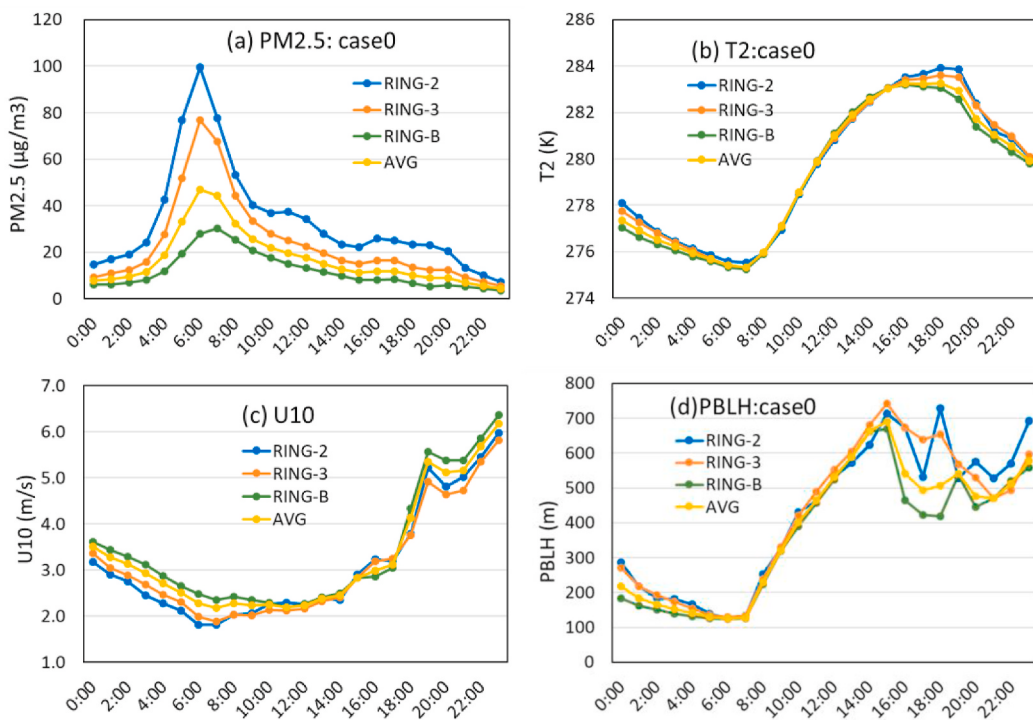


Fig. 2. Diurnal variation curves of (a) PM2.5 concentration, (b) air temperature at 2 m (T2), (c) wind speed at 10 m (U10), (d) planetary boundary layer height (PBLH) in each circle of CASE0.

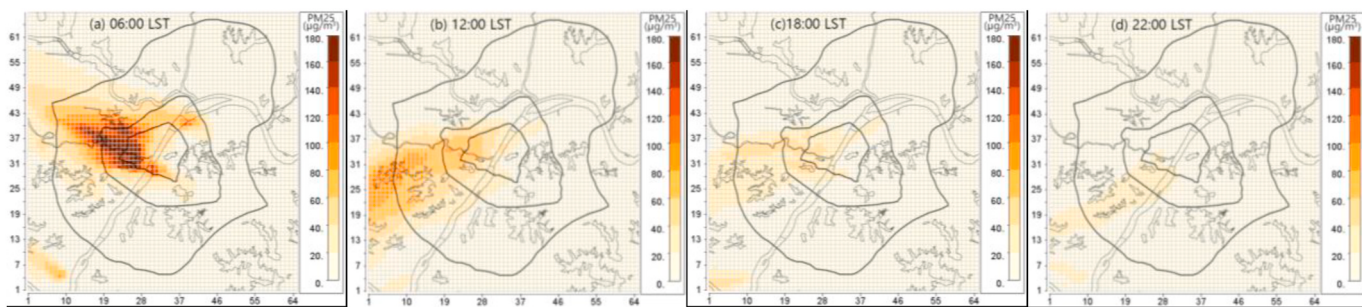


Fig. 3. The spatial distribution of PM_{2.5} concentration of CASE0 at typical times.

3. Spatiotemporal distribution characteristics of PM_{2.5} concentration

3.1. Performance evaluation of numerical mode

The monitoring data of six stations in urban area were selected for comparison with CASE0 to verify the accuracy of the model. Table 1 reflects the correlation coefficient (R), mean error (ME) and root mean square error (RMSE) of the simulated and the observed values of the hourly average PM_{2.5} concentration, air temperature at 2 m (T2), wind speed at 10 m (U10) at the six stations. The verification results show that, the simulated value of T2 is closest to the observed value, followed by U10, and the simulated result of PM_{2.5} concentration is the worst. The R of T2 and U10 at all stations is greater than 0.9 and 0.8 except for two stations HKJT and WCZY. This verification result shows that the WRF simulation result of the weather field is credible. The R of PM_{2.5} concentration of all stations are higher than 0.65, and the R value of WJS station is the lowest ($R = 0.655$), and its ME value and RMSE value are the largest ($14.7 \mu\text{g}/\text{m}^3$ and $18.2 \mu\text{g}/\text{m}^3$, respectively). The simulation results show that the simulated values and observed values show similar trends. However, the simulated values of most stations are lower than the observed values, especially the magnitude and time of peak concentration. The main reason for this phenomenon is that the accuracy of the CMAQ model for PM_{2.5} concentration simulation mainly depends on the accuracy of the emission inventory. However, both the coverage range (nationwide) and grid accuracy (0.25°) of the Multi-resolution Emission Inventory for China (MEIC) used in this study were far beyond the range and accuracy required for numerical simulation of individual cities. Although MEIC can be used by the CMAQ model after temporal and spatial interpolation refinement, the accuracy of the simulation results will be affected. This is also a common problem in the CMAQ model for atmospheric pollution simulation and forecasting in China. Another reason that affects the accuracy of the simulation is that the CMAQ model cannot simulate the meteorological field by itself, but rely on the meteorological field provided by the WRF model. The accuracy of the WRF model will also have an impact on the accuracy of the CMAQ model simulation.

3.2. Temporal distribution characteristics of PM_{2.5} concentration

The mean hourly variation of PM_{2.5} concentration in different areas of Wuhan were calculated within different highway rings (Fig. 2). The results showed that the diurnal variation of PM_{2.5} concentration in Wuhan experienced a process of increasing first and then decreasing, and there was a noticeable peak concentration. Within the second and the third highway rings, the peak concentration of PM_{2.5} appeared at 06:00, and the peak concentration in the beltway ring appeared at 07:00. Due to the absence of solar radiation (the sunrise time in winter of Wuhan is later than 07:00), the underlying surface of the city dissipates heat to the near-ground air in the form of long-wave radiation. The air temperature continuously declined (Fig. 2) and reach the minimum value at 07:00. The decrease in air temperature weakened the

atmospheric turbulence energy, leading U10 and PBLH to continuously decrease to the lowest amount of the whole day around 07:00. The low temperature thereby reduce the rate of horizontal and vertical diffusion of air pollutants, which is the main reason for the rise of PM_{2.5} concentration during this period. At the peak concentration time, the average concentration of PM_{2.5} in Wuhan is about $47 \mu\text{g}/\text{m}^3$. From 06:00 to 08:00, the PM_{2.5} concentration in Wuhan has been at a relatively high level. It's partly due to the weakening of the ability of air pollutants to diffuse. On the other hand, it is also affected by vehicle exhaust emissions during the morning rush hours. After 07:00 in the morning, as the solar radiation increases, the underlying surface absorbs solar radiation and begins to heat up, and heats the air near the ground. The air temperature in the urban canopy began to rise, making the atmospheric turbulence activity intense. At this time, U10 and PBLH in the urban canopy began to increase, which promoted the horizontal and the vertical diffusion of air pollutants. The average concentration of PM_{2.5} in the urban canopy gradually decreased and came to a relatively lower $11.2 \mu\text{g}/\text{m}^3$. From 16:00 to 20:00, due to the weakening of solar radiation, the atmospheric turbulence activity has weakened, which reduced U10 and PBLH. Coupling with the vehicle emissions in the evening rush hours, the average PM_{2.5} concentration increased slightly. However, compared with the concentration at 06:00, U10 and PBLH were still high, the average PM_{2.5} concentration is only about a quarter of the peak. 20:00 later, as U10 and PBLH began to increase again, the average PM_{2.5} concentration gradually decreased.

3.3. Spatial distribution characteristics of PM_{2.5} concentration

The spatial distribution of PM_{2.5} in Wuhan showed a gradually decreasing trend from inner city to the out skirt (Fig. 3). The concentration of PM_{2.5} in the downtown area (within the second ring highway) was the highest and gradually decreased as the downtown area's distance increased. The average PM_{2.5} concentration in the downtown area is 3.3 times that of the beltway ring. This is the most significant spatial characteristic of PM_{2.5} concentration in Wuhan. Comparing U10 and PBLH in different areas, it was found that U10 is the lowest and PBLH is the highest in the second ring highway. This is due to the highest FAR and BH of the second ring highway, which increased the surface roughness length and weakened the wind speed and reduced the horizontal diffusion capacity of PM_{2.5}. On the other hand, the shading effect generated by the higher BD and BH delayed the long-wave radiation in the street canyon and increased the mean air temperature. The higher air temperature increased the atmospheric turbulent energy, promoted the development of the urban boundary layer, and was conducive to the vertical diffusion of PM_{2.5}. The situation is reversed for the beltway ring. The difference in the distribution of PM_{2.5} reflected the two critical ways of PM_{2.5} diffusion: horizontal diffusion mainly depends on the increasing of ventilation capacity, while vertical diffusion required for higher urban boundary layer, which is related to air temperature. The urban morphological indicators such as BH, BD, and UF not only determine the ventilation capacity of the urban area but also change the microclimate and affect local air temperature. It can be seen that those

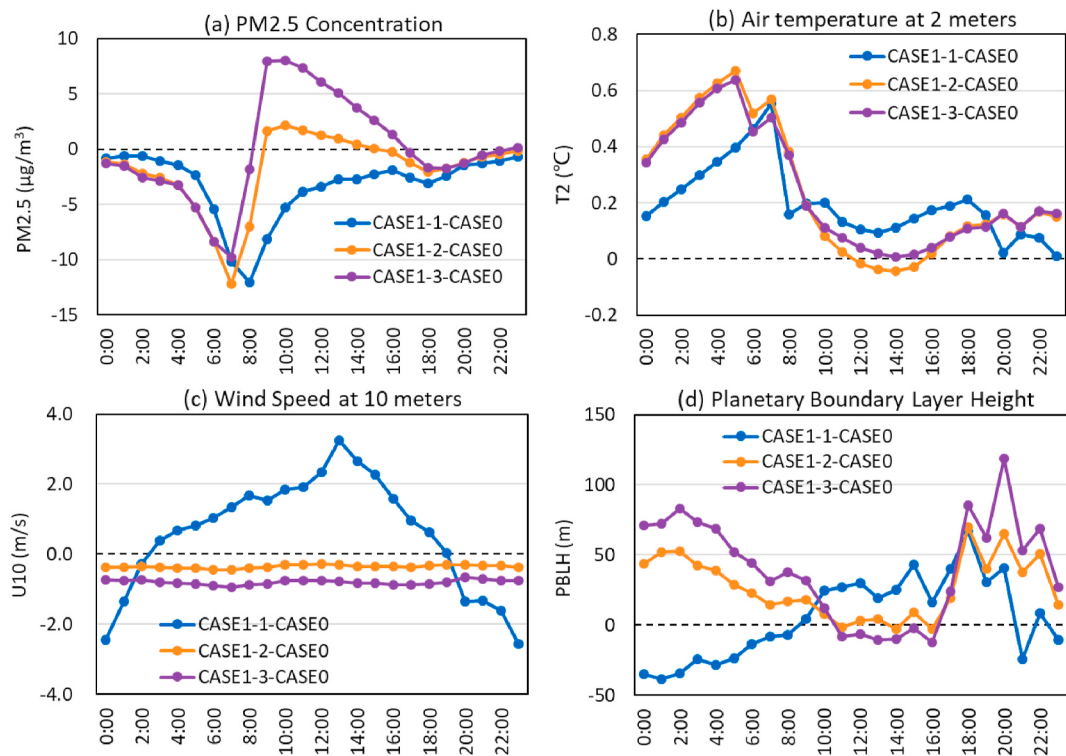


Fig. 4. Diurnal variations of the differences between CASE1 and CASE0 in (a) PM2.5 concentration, (b) T_2 , (c) U_{10} , (d) PBLH.

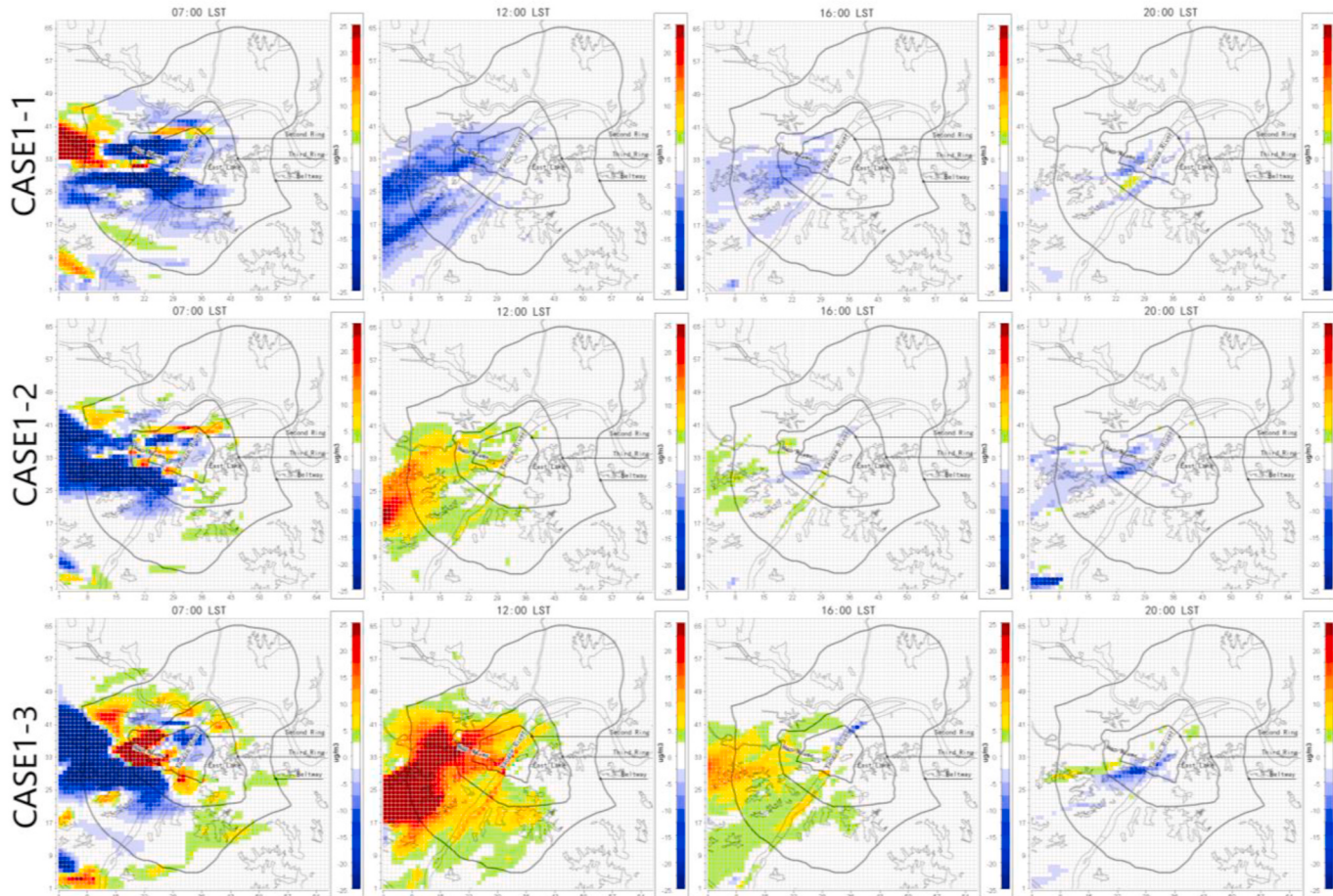


Fig. 5. Comparison of the spatial distribution differences of PM2.5 concentrations in the three cases of CASE1 at typical times.

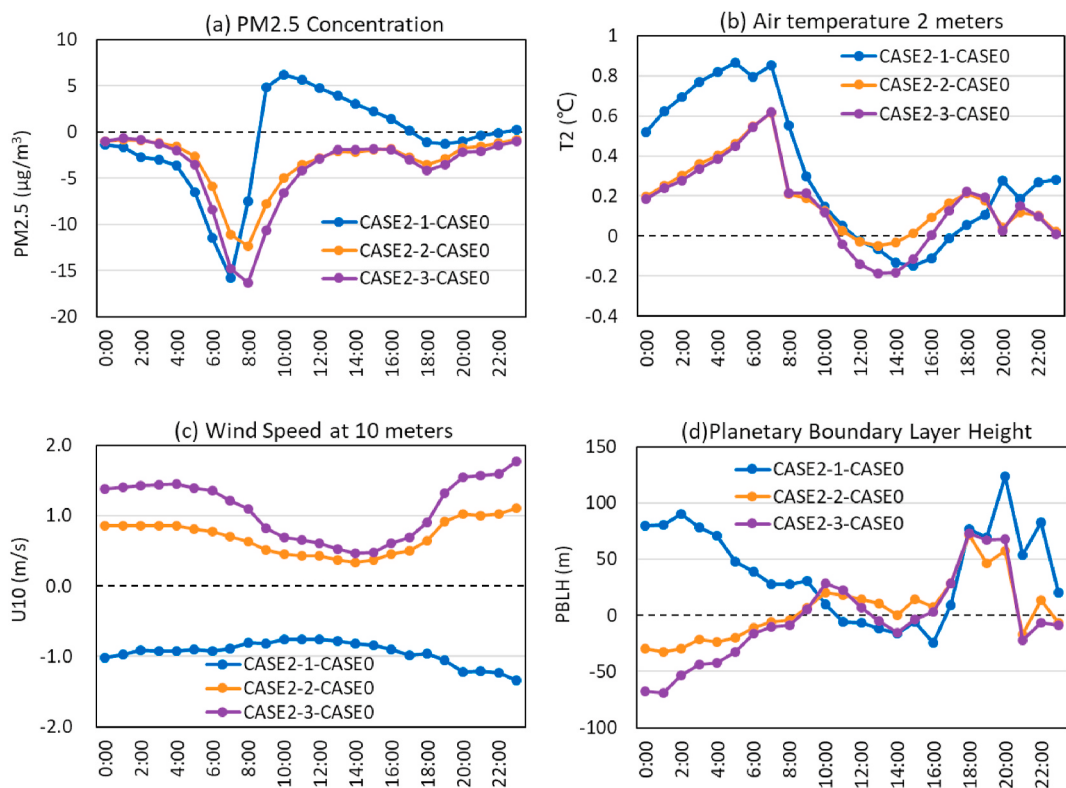


Fig. 6. Diurnal variations of the differences between CASE2 and CASE0 in (a) PM_{2.5} concentration, (b) T₂, (c) U₁₀, (d) PBLH.

urban morphological indicators have a significant influence on the spatial distribution of PM_{2.5} concentration, which deserves more attention from urban planners.

4. Analysis and discussion

The spatial location and emission intensity of emission sources determine the initial spatial and temporal distribution characteristics of PM_{2.5} in urban areas, and the urban form will affect the diffusion process of PM_{2.5}. Therefore, we need to analyze the corresponding changes in PM_{2.5} concentration when urban morphological indicators change. According to their interrelationship, the six indicators were divided into three groups: FAR and BH (CASE1), BD and BW (CASE2), VC and UF (CASE3) and three scenarios were set for each group of indicators. Three cases were set up for each group of morphological indicators by increasing or decreasing their values to assess their sensitivity to PM_{2.5}. For CASE1, we discussed three scenarios of FAR and BH: (1) Compared with CASE0, FAR and BH are reduced by 0.5 units and 10 m respectively. (2) Compared with CASE0, FAR and BH were increased by 0.5 units and 10 m respectively. (3) Compared with CASE0, FAR and BH were increased by 1 unit and 20 m compared with CASE0. The other six similar scenarios were applied in CASE2 and CASE3 (Table 2).

4.1. Influence of FAR and BH on PM_{2.5} concentration

It can be seen from Fig. 4 that compared with CASE0, the PM_{2.5} concentration of the three cases at night all decreased. During the daytime, especially from 09:00 to 16:00, the PM_{2.5} concentration in the central urban area increases with the increase of FAR and BH, because changes in BH will cause changes in temperature, wind speed and the planetary boundary layer height. In the case of constant BD, increasing the BH and FAR will increase the length of the surface roughness and reduce the wind speed in the urban canopy, then weaken the horizontal diffusion of particles. At the same time, the increase in BH may cause the

“shading effect”, which makes the street canyons in the shadow area of the building during the daytime and reduces the solar radiation obtained by the ground, which leads to the reduction of air temperature and PBLH. These are the two main reasons of the PM_{2.5} concentration rising in this period. In the absence of solar radiation at night, the shielding effect causes multiple reflection and absorption of long-wave radiation in the street valley, delays the process of heat dissipation. Since air temperature is one of the key factors affecting the PBLH, changes in air temperature will cause a simultaneous change in PBLH. Therefore, although the U₁₀ of CASE1 is slightly reduced at night, the increase in air temperature and PBLH is conducive to the vertical diffusion of atmospheric pollutants and the reduction of PM_{2.5} concentration.

From the spatial distribution perspective, when the FAR and BH decrease (CASE1-1), the PM_{2.5} concentration in most areas decreases. But when FAR and BH increase (CASE1-2 and CASE1-3), PM_{2.5} during 09:00–16:00 accumulated in a large area in the southwest of the city, and the magnitude rises with the increase in FAR and BH (Fig. 5). This is because in this period, compared with CASE0, CASE1-2 and CASE1-3 have very small changes in U₁₀ and PBLH, which weakens the diffusion of pollutants and causes PM_{2.5} to accumulate in the downwind direction.

4.2. Influence of BD and BW on PM_{2.5} concentration

Figs. 6 and 7 reflect the temporal and spatial changes of PM_{2.5} with BD and BW. Compared with CASE0, the BD of CASE2-1, CASE2-2, and CASE2-3 were reduced by 10%, increased by 10%, and increased by 20% and BW was reduced by 10 m, increased by 10 m, and increased by 20 m, respectively. It can be seen from Fig. 6 that when BD and BW increase, the PM_{2.5} concentration decreases. Conversely, when BD and BW decrease, PM_{2.5} increases during the daytime. The reason for this phenomenon may be that when FAR and BH are constant, the increase of BD and BW leads to a decrease in the distance between buildings, which will cause long-wave radiation in the street valley to be repeatedly reflected and absorbed. The air temperature in the street valley rises due to

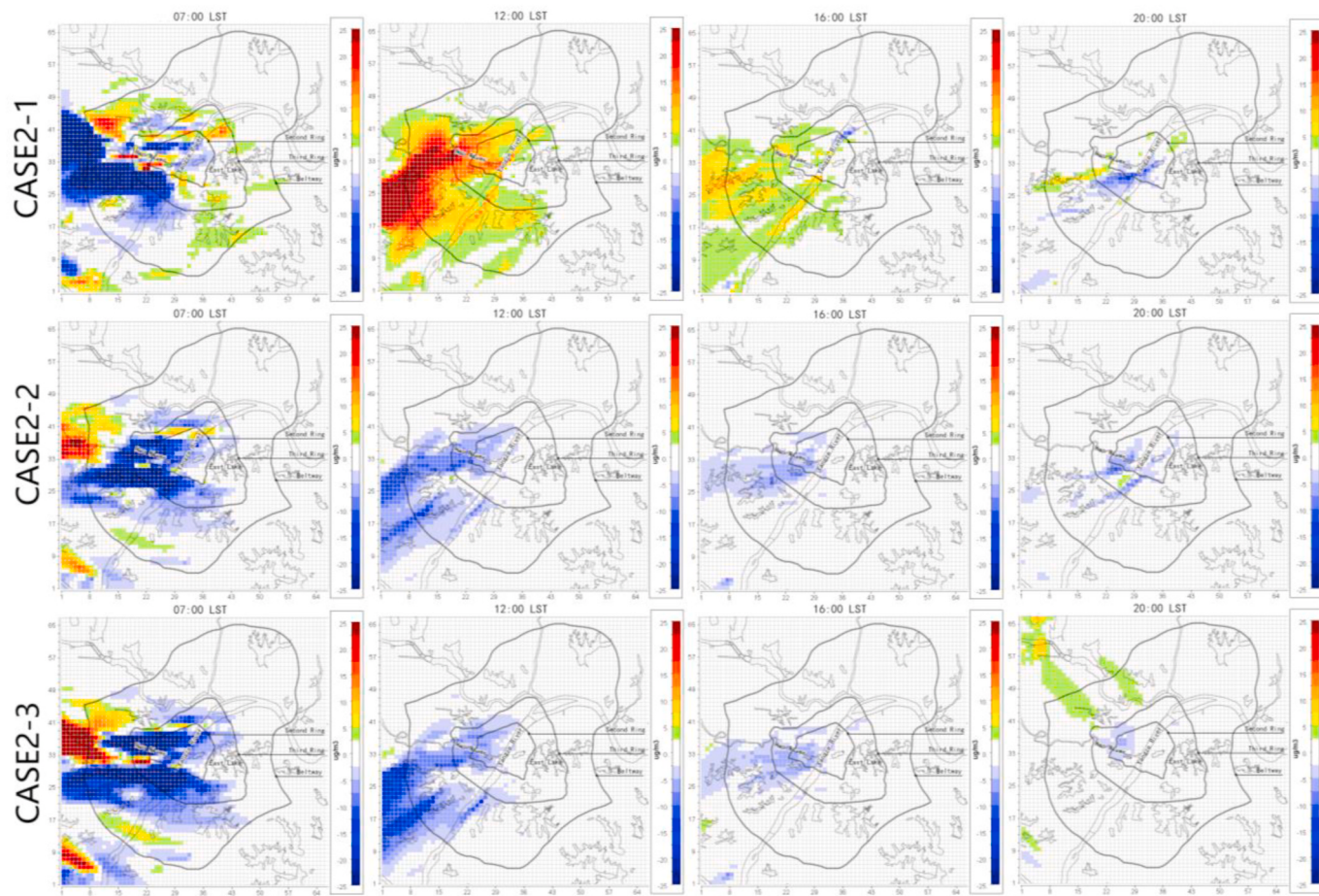


Fig. 7. Comparison of the spatial distribution differences of PM2.5 concentrations in the three cases of CASE2 at typical times.

the accumulation of long-wave radiation and anthropogenic heat rejection, which will increase the aerodynamic energy of atmospheric turbulence and increases the U10 and PBLH. The increase of U10 and PBLH is conducive to the horizontal and vertical diffusion of PM_{2.5}.

From the perspective of the spatial distribution, when BD and BW decrease, the PM_{2.5} concentration has a large area increases during 09:00–16:00 in western of the city, between the third ring and the beltway (Fig. 7). This is mainly because U10 and PBLH of CASE2-1 are smaller than CASE0 in this period, which reduces the horizontal and vertical diffusion capacity of PM_{2.5}.

Comparing the PM_{2.5} spatial and temporal variation of CASE1 and CASE2 (Figs. 4–7), it is found that the four morphological indicators of

FAR, BH, BD, and BW have similar positions of differences in the spatial distribution of PM_{2.5}, but their correlation with PM_{2.5} concentration is just the opposite. This phenomenon may be caused by three reasons. First, the emission time, location, and emission intensity of the pollution sources in the emission inventory determine the temporal and spatial distribution characteristics of PM_{2.5}, and those six cases of CASE1 and CASE2 all use the same emission inventory. Second, the relationships between those four morphological indicators and T2, PM_{2.5} are not a simple linear correlation, but has a threshold. For example, For example, T2 of the three cases of CASE1 is higher than CASE0. When FAR and BH increase to a certain value, they will cause mutual shielding between buildings (shading effect) and reduce the solar radiation obtained on the

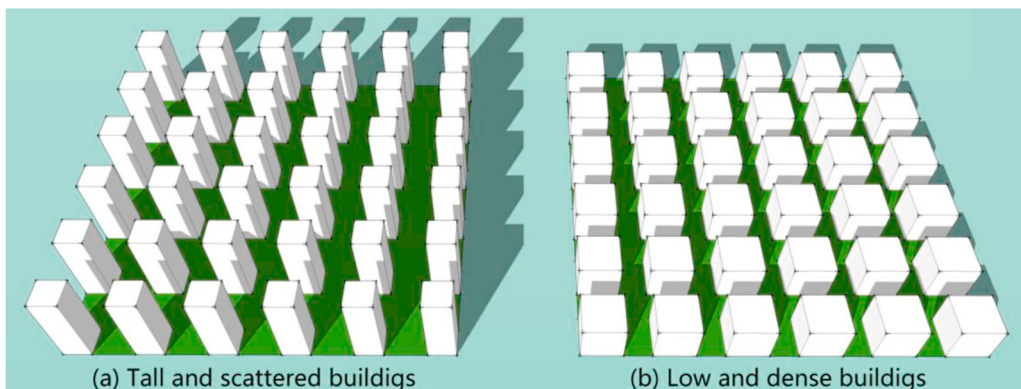


Fig. 8. Two construction mode of city.

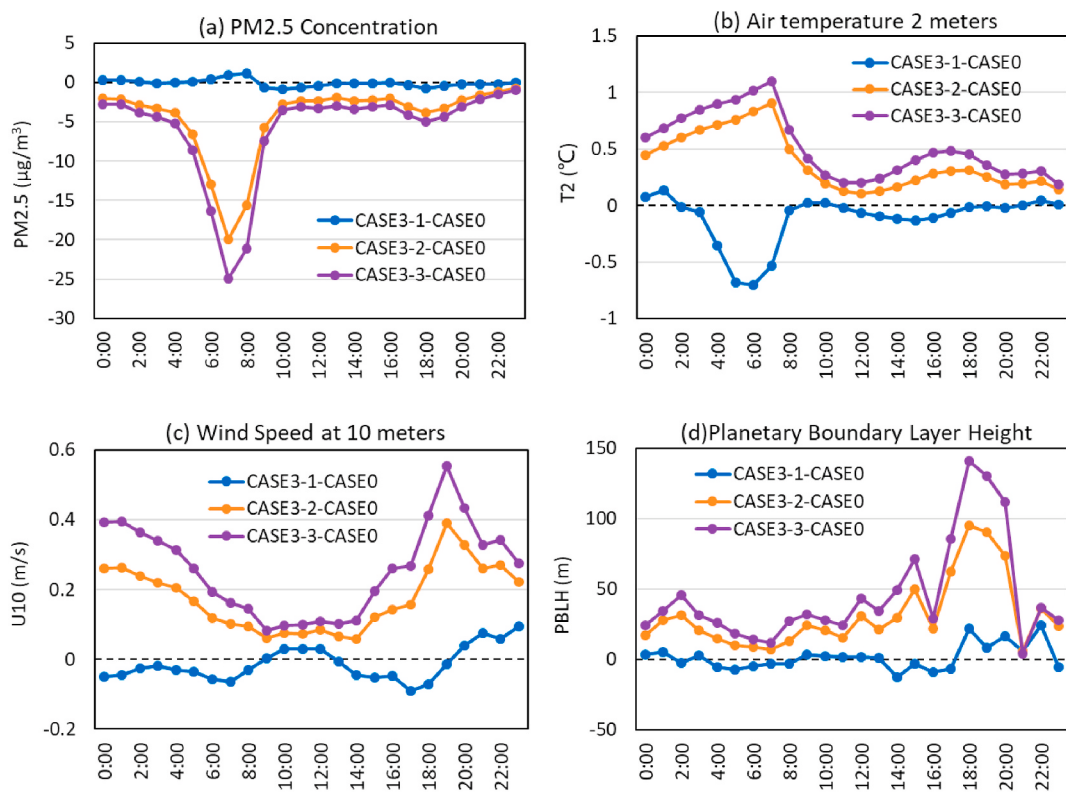


Fig. 9. Diurnal variations of the differences between CASE3 and CASE0 in (a) PM_{2.5} concentration, (b) T₂, (c) U₁₀, (d) PBLH.

ground. But at the same time, the increase of FAR and BH will cause the surface of the street valley to heat up due to multiple reflections and absorptions of long-wave radiation and anthropogenic heat rejection in the block. Although reducing FAR and BH will help the surface to get more solar radiation and heat up, it will also weaken the shielding effect, which is conducive to long-wave radiation heat dissipation. Third, there is a correlation between these four morphological indicators. For example, in CASE1, when FAR and BH decrease, the PM_{2.5} concentration in the southwest of the city decreases. But at the same time, in CASE2, when BD and BW decrease, the concentration of PM_{2.5} in the southwest of the city increases. This shows that there is an opposite correlation between the two sets of morphological indicators.

Generally speaking, when the total amount of urban construction land is certain, planners will first determine the total amount of urban construction by determining the floor area ratio, and then determine the building height, building density, building width and other indicators according to the requirements of lighting and fire protection. Assuming that the area of urban construction land is a fixed value, and the building is abstracted as a box with a side length of BW, the relationship between these four morphological indicators can be expressed by the following formula:

$$S_{building} = FAR \cdot S_{land} \quad (5)$$

$$BD = BW^2 = \frac{3S_{building}}{BH \cdot S_{land}} \quad (6)$$

Where $S_{building}$ is the total area of buildings in the city, S_{land} is the total area of construction land. It can be known from the above formula that when $S_{building}$ is constant, if BH increases, BD and BW decrease accordingly. For planners, this means which model should be chosen when constructing a city? Tall and scattered buildings? Or low and dense buildings? (Fig. 8) These two models have different effects on the urban microclimate and air quality.

4.3. Influence of VC and UF on PM_{2.5} concentration

Three cases were set up to discuss the sensitivity of BD and BW to PM_{2.5} concentration (Table 2). Compared with CASE0, the VC of CASE3-1, CASE3-2, and CASE3-3 were increased by 10%, reduced by 10%, and reduced by 15% and UF was reduced by 10%, increased by 10%, and increased by 20%, respectively. Generally speaking, vegetation has a good ability to adsorb atmospheric particles. When the vegetation coverage decreases, the PM_{2.5} concentration will increase. But CASE3 simulated the opposite result. It can be seen from Fig. 9 that compared with CASE0, when VC and UF increase, the PM_{2.5} concentration decreases, especially at 06:00–08:00, the average PM_{2.5} concentration in the downtown of CASE3-2 and CASE3-3 decrease $-20 \mu\text{g}/\text{m}^3$ and $-25 \mu\text{g}/\text{m}^3$ respectively. The increase in UF means the increase of the artificial underlay surface which makes the surface absorb more solar radiation during the daytime and rises the temperature, thereby increasing the aerodynamic energy of atmospheric turbulence, increasing U₁₀ and PBLH (Fig. 9), and promoting horizontal and vertical diffusion of PM_{2.5}. It is worth noting that the WRF and CMAQ models consider the influence of vegetation on humidity and the precipitation process of particulate matter, but ignore the adsorption of atmospheric particulate matter by plant leaves. This may cause simulation results to differ from expected.

From the perspective of spatial distribution, the variation of PM_{2.5} concentration in the three cases are closely related to the dominant wind direction. When the dominant wind was southeast wind at 00:00 in the morning, the areas with the largest changes in PM_{2.5} concentration in the three cases all appeared in the northwest of the city (Fig. 10). When the dominant wind direction changed to east at 06:00 in the morning, the areas with the largest changes in PM_{2.5} concentration in the three cases were also concentrated in the west of the city. In the afternoon and evening, the prevailing wind direction changed to northeast. At this time, the areas which have the biggest magnitude of PM_{2.5} have changed to the southwest of the city accordingly. This rule is also reflected in section 4.1 and section 4.2.

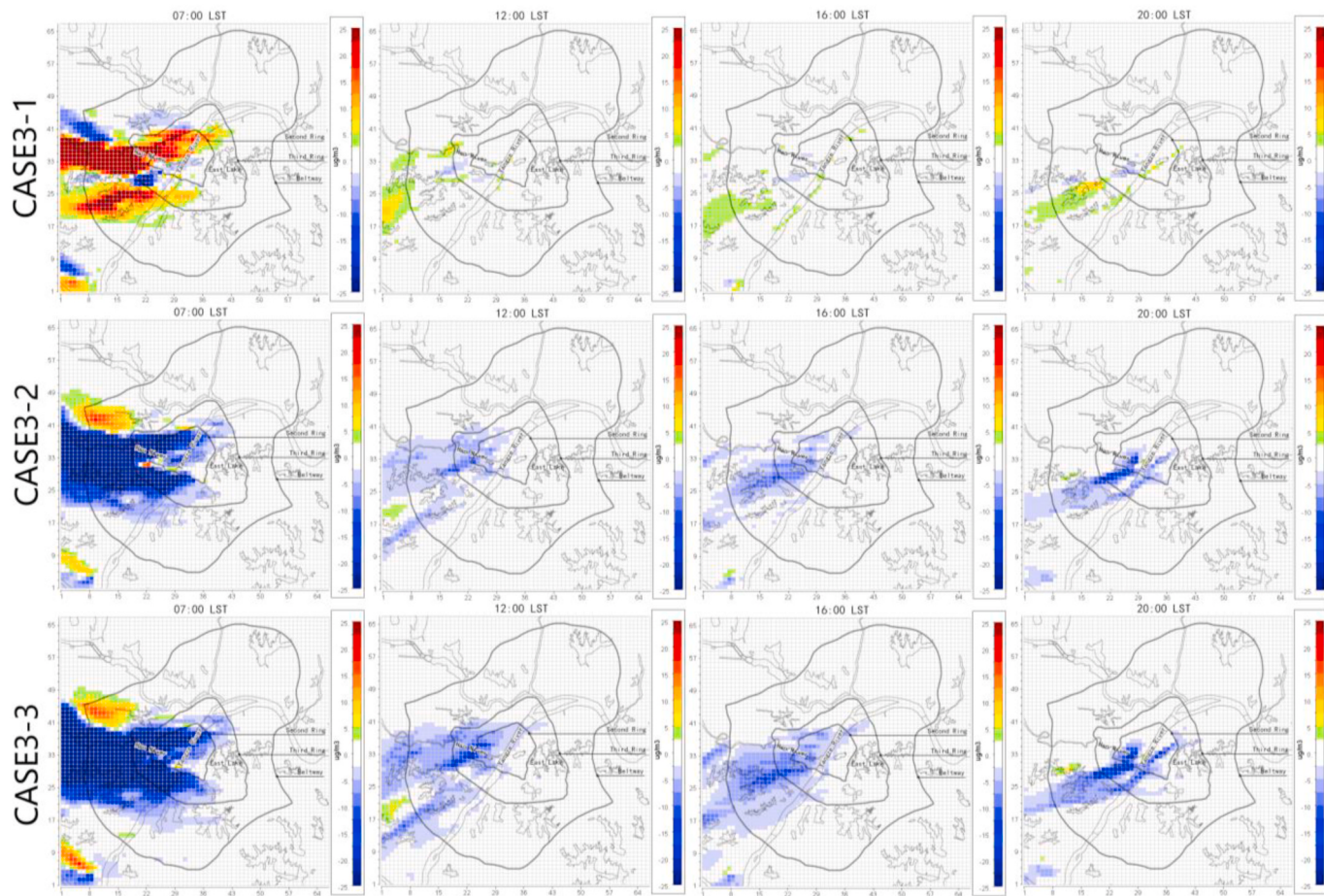


Fig. 10. Comparison of the spatial distribution differences of PM_{2.5} concentrations in the three cases of CASE3 at typical times.

5. Conclusion

With the acceleration of urbanization, most Chinese cities are facing severe air pollution problems. The most effective way to solve the air pollution problem is undoubtedly to reduce the emission of air pollutants from the source, but this method will inevitably have a tremendous negative impact on economic development. Another method is to increase the diffusion capacity of air pollutants by adjusting the urban form to achieve the purpose of reducing the concentration of air pollutants in urban areas. From the perspective of urban planning, this study analyzed the influence mechanism of three groups of urban morphological indicators on the spatial and temporal distribution of PM_{2.5}, including FAR, BH, BD, BW, VC, and UF, with the help of numerical simulations. The main conclusions are drawn in the following aspects:

First, the urban morphology affects PM_{2.5} concentration mainly by changing the urban microclimate. First of all, the change in urban morphology affects the absorption and reflection of long-wave and short-wave radiation on the underlying surface, breaking the energy balance, and making the air temperature in near-surface increase or decrease. Changes in air temperature will cause changes in the atmospheric boundary layer, thereby affecting the vertical diffusion capacity of air pollutants. Of course, it will also cause complex photochemical reactions of air pollutants by the variation of air temperature, but this is not the content that will be discussed in this study. Secondly, the variations of BH and BD will change the roughness length of the underlying surface. While the roughness length is a critical morphological index that affects wind speed and determines the size of wind speed in the urban canopy, which will be related to the horizontal diffusion ability of

air pollutants.

Secondly, according to the results of this study, the increase of FAR, BH, and VC will cause the increase of PM_{2.5} concentration, and the increase of BD, BW, and UF can reduce the PM_{2.5} concentration, especially during rush hours (06:00–08:00 in the morning). Under the same change magnitude, UF has the most obvious impact on PM_{2.5} concentration. This result shows that adopting a compact urban form, reducing BH, increasing BD, BW and UF will help improve urban air quality. This conclusion will help planners to make more reasonable choices when formulating indicators for urban construction.

Finally, this study chose Wuhan in winter as the research object because Wuhan is in a period of large-scale urban construction and rapid expansion. It can also represent the urban development process that most Chinese cities which have gone or are going through. Also, the haze problem in Wuhan in winter is much more severe than that in other seasons. It is worth noting that this study only discussed PM_{2.5} concentration in the urban area of Wuhan, and does not consider other urban environmental issues such as the heat island effect. Therefore, the analysis process and the conclusions are focused on reducing the PM_{2.5} concentration in the urban area. For example, although the concentration of PM_{2.5} can be reduced by increasing BD, it may also increase air temperature and urban heat island effect in the urban area. Therefore, in the follow-up study, more cities and more seasons will be included in the discussion.

Credit author statement

Xu Huahua: simulation, Writing, Visualization, Investigation, Software, Editing. Chen Hong: Conceptualization, Methodology,

Supervision.

Fundings

This work is supported by the following funds:

1. The National Natural Science Foundation of China [grant number 51778251].
2. The National Natural Science Foundation of China [grant number 51538004].

Declaration of competing interest

The authors declare that they have no known competing financial interests or personal relationships that could have appeared to influence the work reported in this paper.

Appendix A. Supplementary data

Supplementary data to this article can be found online at <https://doi.org/10.1016/j.jenvman.2021.112427>.

References

- Aldabe, J., Elustondo, D., Santamaría, C., et al., 2011. Chemical characterisation and source apportionment of PM_{2.5} and PM₁₀ at rural, urban and traffic sites in Navarra (North of Spain). *Atmos. Res.* 102 (1–2), 191–205.
- Aw, Kleeman, 2003. Evaluating the first-order effect of intra-annual temperature variability on urban air pollution. *Journal of Geophysics Research Atmospheres* 108 (D12).
- Banks, R.F., Baldasano, J.M., 2016. Impact of WRF model PBL schemes on air quality simulations over Catalonia, Spain. *Sci. Total Environ.* 572, 98–113.
- Buckley, J.P., Richardson, D.B., 2012. Seasonal modification of the association between temperature and adult emergency department visits for asthma: a case-crossover study. *Environ. Health (Lond.)* 11, 55.
- Buyantuyev, A., Wu, J., Gries, C., 2015. Multi-scale analysis of the urbanization pattern of the Phoenix metropolitan landscape of USA: time, space and thematic resolution. *Landsc. Urban Plann.* 94 (3–4), 206–217.
- Chen, F., Dudhia, J., 2001. Coupling an advanced land surface hydrology model with the penn state/NCAR MM5 modeling system. Part I: model implementation and sensitivity. *Mon. Weather Rev.* 129, 569–585.
- Chen, F., Kusaka, H., Tewari, M., et al., 2004. Utilizing the coupled WRF/LSM urban modeling system with detailed urban classification to simulate the urban heat island phenomena over the greater Houston area. In: Fifth Conf. On Urban Environment. Amer Meteor Soc, Vancouver, BC, Canada.
- Chen, Y., Li, X., Zheng, Y., et al., 2011. Estimating the relationship between urban forms and energy consumption: a case study in the Pearl River Delta, 2005–2008. *Landsc. Urban Plann.* 102 (1), 33–42.
- Chen, Z., Zhu, Y., Wang, Y., et al., 2014. Association of meteorological factors with childhood viral acute respiratory infections in subtropical China: an analysis over 11 years. *Arch. Virol.* 159 (4), 631–639.
- Chen, M., Dai, F., Yang, B., et al., 2019a. Effects of urban green space morphological pattern on variation of PM_{2.5} concentration in the neighborhoods of five Chinese megacities. *Build. Environ.* 158, 1–15.
- Chen, X., Zhao, P., Hu, Y., et al., 2019b. Canopy transpiration and its cooling effect of three urban tree species in a subtropical city- Guangzhou, China. *Urban For. Urban Green.* 43, 126368.
- Dawson, J.P., Adams, P.J., Pandis, S.N., 2007. Sensitivity of PM_{2.5} to climate in the Eastern US: a modeling case study. *Atmos. Chem. Phys.* 7 (16), 4295–4309.
- Gunawardena, K.R., Wells, M.J., Kershaw, T., 2017. Utilising green and blue-space to mitigate urban heat island intensity. *Sci. Total Environ.* 584–585, 1040–1055.
- Guo, L., Luo, J., Yuan, M., et al., 2019. The influence of urban planning factors on PM_{2.5} pollution exposure and implications: a case study in China based on remote sensing, LBS, and GIS data. *Sci. Total Environ.* 659, 1585–1596.
- He, X., Lin, Z., 2017. Interactive effects of the influencing factors on the changes of PM_{2.5} concentration based on GAM Model. *Environ. Sci.* 38 (1), 22–32.
- Hong, S.Y., Lim, J.O.J., 2006. The WRF single-moment 6-class microphysics scheme (WSM6). *Asia Pacific Journal of Atmospheric Sciences* 42, 129–151.
- Hong, S.Y., Noh, Y., Dudhia, J., 2006. A new vertical diffusion package with an explicit treatment of entrainment processes. *Mon. Weather Rev.* 134, 2318–2341.
- Hu, J., Chen, J., Yang, Q., et al., 2016. One-year simulation of ozone and particulate matter in China using WRF/CMAQ modeling system. *Atmos. Chem. Phys.* 16, 10333–10350.
- Huang, H., Yang, H., Deng, X., et al., 2019. Influencing mechanisms of urban heat island on respiratory diseases. *Iran. J. Public Health* 48 (9), 1636–1646.
- Jeanjean, A., Monks, P.S., Leigh, R.J., 2016. Modelling the effectiveness of urban trees and grass on PM_{2.5} reduction via dispersion and deposition at a city scale. *Atmos. Environ.* 147, 1–10.
- Kang, J.E., Song, S.K., Lee, H.W., et al., 2012. The influence of meteorological conditions and complex topography on Ozone concentrations in a valley area near coastal metropolitan cities. *Terr. Atmos. Ocean Sci.* 23 (1), 25–38.
- Kang, Y., Song, S., Hwang, M., et al., 2016. Impacts of detailed land-use types and urban heat in an urban canopy model on local meteorology and Ozone levels for air quality modeling in a coastal city, Korea. *Terr. Atmos. Ocean Sci.* 27 (6), 877–891.
- Kusaka, H., Kimura, F., 2004. Thermal effects of urban canyon structure on the nocturnal heat island: numerical experiment using a mesoscale model coupled with an urban canopy model. *J. Appl. Meteorol.* 43, 1899–1910.
- Kusaka, H., Kondo, H., Kikegawa, Y., et al., 2001. A simple single layer urban canopy model for atmospheric models: comparison with Multi-layer and Slab models. *Boundary-Layer Meteorol.* 101, 329–358.
- Ma, J., Liu, Z., Chai, Y., 2015. The impact of urban form on CO₂ emission from work and non-work trips: the case of Beijing, China. *Habitat Int.* 47, 1–10.
- Masson, V., 2000. A physically-based scheme for the urban energy budget in atmospheric models. *Boundary-Layer Meteorol.* 94, 357–397.
- Miao, S., Chen, F., Lemone, M.A., et al., 2009. An observational and modeling study of characteristics of urban heat island and boundary layer structures in Beijing. *J Appl Meteorol Climatol* 48, 484–501.
- Mlawer, E.J., Taubman, S.J., Brown, P.D., et al., 1997. Radiative transfer for inhomogeneous atmosphere: RRTM, a validated correlated-k model for the long-wave. *J. Geophys. Res.* 102, 16663–16682.
- Ohara, T., Akimoto, H., Kurokawa, J., et al., 2007. An Asian emission inventory of anthropogenic emission sources for the period 1980–2020. *Atmos. Chem. Phys.* 7 (16), 4419–4444.
- Ou, J., Liu, X., Li, X., et al., 2013. Quantifying the relationship between urban forms and carbon emissions using panel data analysis. *Landscape Ecol.* 28 (10), 1889–1907.
- Rasanen, J., Holopainen, T., Joutsensuu, J., et al., 2013. Effects of species-specific leaf characteristics and reduced water availability on fine particle capture efficiency of trees. *Environ. Pollut.* 183, 64–70.
- Saebo, A., Popek, R., Nawrot, B., et al., 2012. Plant species differences in particulate matter accumulation on leaf surfaces. *Sci. Total Environ.* 427, 347–354.
- Shi, Y., Lau, K.L., Ng, E., 2016. Developing street-level PM_{2.5} and PM₁₀ land use regression models in high-density Hong Kong with urban morphological factors. *Environ. Sci. Technol.* 8178–8187.
- Shi, K., Wang, H., Yang, Q., et al., 2019. Exploring the relationships between urban forms and fine particulate (PM_{2.5}) concentration in China: a multi-perspective study. *J. Clean. Prod.* 231 (SEP.10), 990–1004.
- Shi, K., Li, Y., Chen, Y., et al., 2019a. How does the urban form-PM_{2.5} concentration relationship change seasonally in Chinese cities? A comparative analysis between national and urban agglomeration scales. *J. Clean. Prod.* 239, 118088.
- Tai, A.P.K., Mickley, L.J., Jacob, D.J., 2010. Correlations between fine particulate matter (PM_{2.5}) and meteorological variables in the United States: implications for the sensitivity of PM_{2.5} to climate change. *Atmos. Environ.* 44 (32), 3976–3984.
- Tham, J., Sarkar, S., Jia, S., et al., 2019. Impacts of peat-forest smoke on urban PM_{2.5} in the Maritime Continent during 2012–2015: carbonaceous profiles and indicators. *Environ. Pollut.* 248 (MAY), 496–505.
- Wang, Y.S., Yao, L., Wang, L.L., et al., 2014. Mechanism for the formation of the January 2013 heavy haze pollution episode over central and eastern China. *Sci. China Earth Sci.* 57 (1), 14–25.
- Wang, H., Wang, Y., Yang, J., et al., 2015. Multi-scale comparisons of particulate matter and its size fractions deposited on leaf surfaces of major greening tree species. *Scientia Silvae Sinicae*, 07.
- Wuhan Municipal Bureau of Statistics, 2016. Wuhan Statistical Yearbook -2016. China Statistics Press, Beijing.
- Yin, C., Yuan, M., Lu, Y., et al., 2018. Effects of urban form on the urban heat island effect based on spatial regression model. *Sci. Total Environ.* 634 (SEP.1), 696–704.
- Zeng, Y., Chen, Y., Guo, H., et al., 2018. Influencing factors of urban lake wetland of built environment on air PM₁₀/PM_{2.5} concentration- A case of Wuhan. *Chinese Landscape Architecture* 34 (7), 104–109.
- Zhou, B., Rybski, D., Kropp, J.P., 2017. The role of city size and urban form in the surface urban heat island. *Science Report-UK* 7, 4791.